A model for measurement of the states in a coupled-dot qubit

2009 J. Phys.: Condens. Matter 21 125301

(http://iopscience.iop.org/0953-8984/21/12/125301)

IOP PUBLISHING JOURNAL OF PHYSICS: CONDENSED MATTER

J. Phys.: Condens. Matter **21** (2009) 125301 (5pp) doi:10.1088/0953-8984/21/12/125301

A model for measurement of the states in a coupled-dot qubit

H B Sun and H M Wiseman

Centre for Quantum Computer Technology, Centre for Quantum Dynamics,
Griffith University, Brisbane 4111 QLD, Australia

E-mail: h.sun@griffith.edu.au

Received 12 September 2008, in final form 23 December 2008
Published 26 February 2009
Online at stacks.iop.org/JPhysCM/21/125301

Abstract

We propose a quantum trajectory analysis of a scheme to measure the states of a coupled-dot device (qubit) where there is a fluctuating energy gap Δ between the two states. The system consists of the qubit and a readout dot coupled to source and drain leads. The tunnel rate through the detector is conditioned by the occupation number of the nearer quantum dot (target) of the qubit and therefore probes the states of the qubit. We derive a Lindblad-form master equation to calculate the unconditional evolution of the qubit and a conditional stochastic master equation calculating the conditional evolution for different tunneling rates. The results show the effects of various device parameters and provide the optimum selection and combination of the system structure.

1. Introduction

There has been wide interest and numerous proposals in the area of quantum transport and measurement in mesoscopic electronic systems both theoretically [1–9] and experimentally [10–12]. Coupled quantum dots have been suggested as qubits: the basic element of a quantum computer. In addition to manipulations of quantum states, a readout device is required to perform quantum measurements of the resulting state of the qubit. The accurate readout of data encoded in the qubit states is an important part of the performance of a quantum computer. There have been interesting reports on relevant experiments, for instance, measuring current tunneling through a quantum dot [12], detecting bidirectional flowing electrons [11], and projective readout of dephasing time in coupled electron spins [10].

In this paper, we apply the quantum trajectory theory, introduced for open systems in quantum optics in [13], to the problem of monitoring a coupled quantum dot system. The system is coupled to an apparatus which includes a bath or reservoir (the source and drain leads). This coupling takes place via unitary quantum evolution, and tracing over the apparatus results in a mixed state for the system. Quantum trajectory theory is based on applying the measurement postulate of quantum mechanics to the apparatus. The measurement process reveals information about the system (and apparatus), and one can calculate a density matrix ρ for the system which is conditioned on the results of observation of the apparatus. This state is more pure than the unconditioned state, but is still not pure in general. This procedure introduces a statistical element into the system dynamics—the conditioned ρ evolves stochastically. We assume that in the absence of measurement (or averaging over the measurement results), the irreversible evolution is described by a Lindblad master equation [14]. This ensures that, even with the measurement included, the stochastic master equation [12] still preserves the three basic properties of the density matrix: positivity, Hermiticity and norm. By contrast, as we showed in [8], some commonly used master equations for the regime of the readout device (RD) operating in sequential-tunneling are not of the Lindblad form.

We derive a Lindblad-form master equation and a corresponding conditional stochastic master equation to describe the conditioned evolution of a qubit under weak continuous measurement. The detector is a quantum tunneling RD such as the quantum contact point, single electron transistor, or quantum dot coupled to source and drain leads. The measured system is a coupled quantum dot or charge qubit. Unlike previous related work [4], we do not assume that the qubit energy levels are degenerate. This leads to quite different behavior in the stochastic trajectories of the system. The ensemble-averaged evolution of the qubit state is also calculated for various parameter combinations to estimate the optimum selection.

The paper is organized as follows. In section 2 we introduce the system and modeling followed by section 3 calculating trajectories in the cases without and with a variable energy gap between the two dot states. We discuss the results and parameter comparison with reported experimental data in section 4, and summarize in section 5.

2. The system and modeling

The system studied is depicted schematically in figure 1. The charge qubit consists of two spatially separated quantum dots, which are strongly coupled. There is only one single electronic bound state that can be occupied in each dot of the qubit. A single excess electron is shared by the coupled-quantum-dot. The energy difference between these two bound states is Δ and the electron can tunnel between two dots at rate t. The RD determines the presence of the electron on one of the dots, for example dot 1 in the diagram (as the target). The interaction between the target and RD changes the current flowing through the RD. That is, in the RD the electron-tunneling rate is conditioned on the occupation of the target dot at D_0 and $D_0 + D_1$ for non-occupied and occupied cases, respectively.

The total Hamiltonian of the qubit system for the coherent coupling case ($\Delta = 0$) is

$$H = \hbar \sum_{i=1}^{2} \omega_i c_i^\dagger c_i + \mathrm{i}\hbar \frac{t}{2}(c_1^\dagger c_2 - c_2^\dagger c_1), \tag{1}$$

where $c_i^\dagger, c_i$ represent the Fermi annihilation and creation operators for the single electron state of the ith dot and t is the tunneling rate between two dot states. For the readout device, the background tunneling current, when the target is not occupied, is D_0, and the rate of the detected signal of the occupation of the target is $D_0 + D_1$ with $D_1 > 0$. We assume that the tunneling through the RD is one way only ($\downarrow$ direction as shown in figure 1) and the escaping tunneling rate from the center island to the drain is large compared to other rates (e.g. the entry rate from the source to the center island). Based on these assumptions we can derive a Lindblad-form 'master equation [4]:

$$\frac{\mathrm{d}\rho}{\mathrm{d}t} = -\mathrm{i}[H, \rho] + \gamma_{\mathrm{dec}}\{c_1^\dagger c_1 \rho c_1^\dagger c_1 - \tfrac{1}{2}[c_1^\dagger c_1 c_1^\dagger c_1 \rho + \rho c_1^\dagger c_1 c_1^\dagger c_1]\},$$

where $\gamma_{\mathrm{dec}} = 2D_0 + D_1$ is the decoherence rate. The stochastic record of measurement comprises a sequence of times at which electrons tunnel through the RD. In the zero response-time limit, the current consists of a sequence of δ function spikes: $i(t) = e\,\mathrm{d}N/\mathrm{d}t$ where $\mathrm{d}N(t)$ is a classical point process defined by the following conditions

$$\begin{aligned} [\mathrm{d}N(t)]^2 &= \mathrm{d}N(t) \\ E[\mathrm{d}N(t)]/\mathrm{d}t &= D_0 + D_1 \mathrm{Tr}[c_1^\dagger c_1 \rho_{\mathrm{c}}(t) c_1^\dagger c_1], \end{aligned} \tag{2}$$

where $E[x]$ indicates a classical average of a classical stochastic process x. The first condition states that $\mathrm{d}N(t)$ equals zero or one. The second means that the rate of events

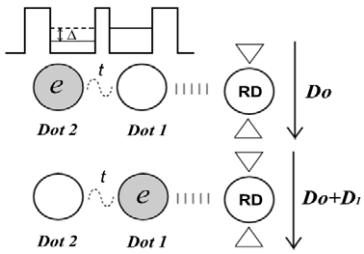

Figure 1. Illustration of the system.

is equal to the quiescent rate D_0 plus an additional rate D_1 if and only if the electron is in the target dot. Applying the *theory of open quantum systems* [13], we obtain the stochastic master equation conditioned on the observed event in time $\mathrm{d}t$ as [4]

$$\begin{aligned} \mathrm{d}\rho_{\mathrm{c}} = \mathrm{d}N \left[\frac{D_0 + D_1 \mathcal{T}[c_1^\dagger c_1] + 2D_0 \mathcal{D}[c_1^\dagger c_1]}{D_0 + D_1 \mathrm{Tr}[\rho_{\mathrm{c}} c_1^\dagger c_1]} - 1 \right] \rho_{\mathrm{c}} \\ + \mathrm{d}t \left[\frac{-D_1}{2}\{c_1^\dagger c_1, \rho_{\mathrm{c}}\} + D_1 \mathrm{Tr}[\rho_{\mathrm{c}} c_1^\dagger c_1]\rho_{\mathrm{c}} - \mathrm{i}[H, \rho_{\mathrm{c}}] \right] \end{aligned} \tag{3}$$

where $\mathcal{T}[A]B = ABA^\dagger$, $\{A, B\} = AB + BA$ and $\mathcal{D}[A]B = \mathcal{T}[A]B - (A^\dagger AB + BA^\dagger A)/2$.

3. Calculations

3.1. Coherent tunneling case

To simplify the calculations we introduce the Bloch representation of the state matrix:

$$\rho = \tfrac{1}{2}(I + x\sigma_x + y\sigma_y + z\sigma_z). \tag{4}$$

The Pauli matrices are defined as

$$\begin{aligned} \sigma_x = c_1^\dagger c_2 + c_2^\dagger c_1, \qquad \sigma_y = \mathrm{i}(c_2^\dagger c_1 - c_1^\dagger c_2), \\ \sigma_z = c_2^\dagger c_2 - c_1^\dagger c_1. \end{aligned} \tag{5}$$

The moments of the Pauli matrices are given by $\langle \sigma_\alpha \rangle = \alpha$ ($\alpha = x, y, z$), which provide physical meanings. For example, when the system is in a definite state (dot 1 or dot 2), the average population difference z is equal to ± 1. The set of coupled stochastic differential equations for the Bloch sphere variables can be expressed as

$$\begin{aligned} \mathrm{d}x_{\mathrm{c}} &= \left(-t \cdot Z_{\mathrm{c}} - \frac{D_1}{2} z_{\mathrm{c}} x_{\mathrm{c}} \right) \mathrm{d}t - x_{\mathrm{c}} \mathrm{d}N(t), \\ \mathrm{d}y_{\mathrm{c}} &= -\frac{D_1}{2} z_{\mathrm{c}} y_{\mathrm{c}}\, \mathrm{d}t - y_{\mathrm{c}}\, \mathrm{d}N(t), \\ \mathrm{d}z_{\mathrm{c}} &= \left[t x_{\mathrm{c}} + \frac{D_1}{2}(1 - z_{\mathrm{c}}^2) \right] \mathrm{d}t - \left[\frac{D_1(1 - z_{\mathrm{c}}^2)/2}{D_0 + D_1(1 - z_{\mathrm{c}}^2)/2} \right]. \end{aligned} \tag{6}$$

Detailed derivation and approximations are referred to in [4]. The subscript c indicates that these variables refer to the conditional state. Calculated trajectories at various coupling rates when $D_0 = 0$ are plotted in figure 2. When the coupling between the dots is small ($t < \gamma_{\mathrm{dec}}/2$) the electron is located in a fixed dot ($z = -1$ at dot 2 and $z = +1$ at dot 1) for a

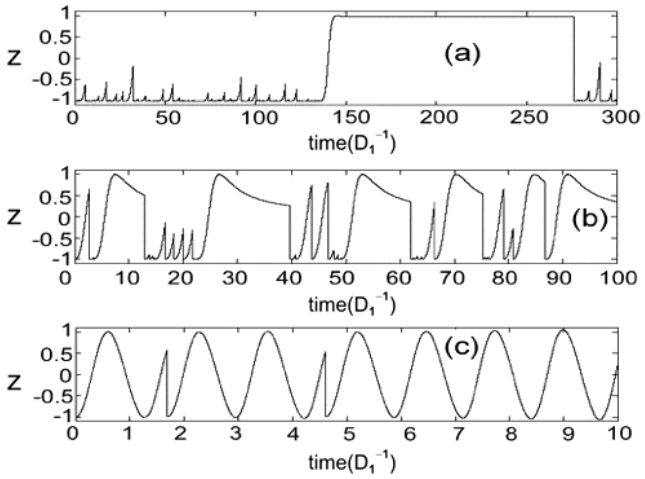

Figure 2. Trajectories for various coupling rates: $t =$ (a) 0.1; (b) 0.5; (c) $5D_1$.

long time until a sudden transition, as shown in figure 2(a). For the strong coupling case, as shown in figure 2(c) when $t \gg \gamma_{\rm dec}/2$, the trajectory shows nearly sinusoidal oscillations with jumps occurring at an average rate of $\gamma_{\rm dec}/2$, this means that the electron is not localized but shared by two dots through the strong tunneling. In figure 2(b), with the moderate coupling strength, the trajectory shows that the electron is neither well localized nor regular harmonically oscillating between two dots.

3.2. Energy gap $\Delta \neq 0$ case

We extend the application to the case where there is an energy difference of $\Delta \neq 0$ between two dot states, which is a model of, for example, the qubit system proposed by Kane [15]. The relevant Hamiltonian can be written as $H = \left(\begin{smallmatrix} \Delta & t \\ t & 0 \end{smallmatrix}\right)$, where t is the tunneling between two states. The stochastic differential equations for the Bloch sphere variables describing conditional dynamics now become

$$\mathrm{d}x_{\rm c} = \left(-tz_{\rm c} - y_{\rm c}\Delta - \frac{D_1}{2}x_{\rm c}z_{\rm c}\right)\mathrm{d}t - x_{\rm c}\,\mathrm{d}N(t)$$

$$\mathrm{d}y_{\rm c} = \left(x_{\rm c}\Delta - \frac{D_1}{2}y_{\rm c}z_{\rm c}\right)\mathrm{d}t - y_{\rm c}\,\mathrm{d}N(t)$$

$$\mathrm{d}z_{\rm c} = \left(tx_{\rm c} + \frac{D_1}{2}(1-z_{\rm c}^2)\right)\mathrm{d}t - \frac{D_1(1-z_{\rm c}^2)/2}{D_0 + D_1(1-z_{\rm c}^2)/2}\,\mathrm{d}N(t). \tag{7}$$

The numerical calculation results are presented in figure 3. By comparison with figure 2 one can see the effect of the energy gap. It takes a much longer time to tunnel through the gap from one dot to the other for the low tunneling rate case (note: the timescales on the horizontal axes are different in these two figures) while quasi-harmonic oscillation features are kept in the high tunneling rate region (tunneling rate $t \gg$ gapΔ). For the moderate coupling rate, the plot shows non-localization and non-sinusoidal oscillations between two dots with lower frequency compared to those in figure 2.

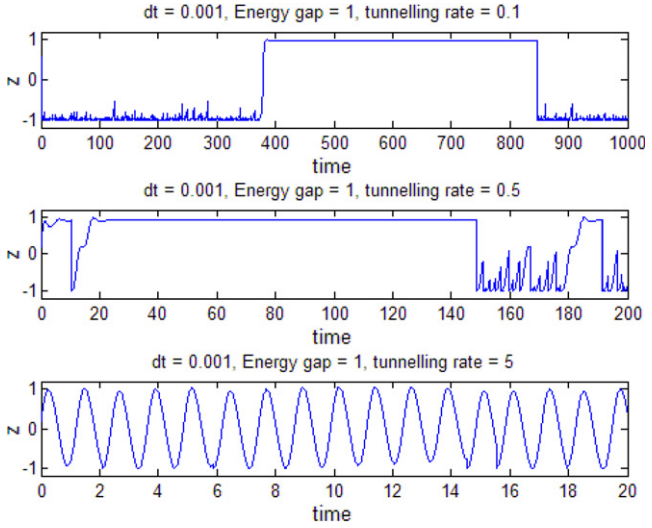

Figure 3. Trajectories for various t with $\Delta = 1$, the parameters are shown on top of each plot and the rates are all normalized by D_1. (This figure is in colour only in the electronic version)

In order to investigate the influences of various parameters of devices on the system dynamics (performance) we investigate the unconditional ensemble average properties of the system in detail.

3.3. Ensemble average properties

The relevant Hamiltonian can be diagonalized by rotating by an angle of $\theta = \frac{1}{2}tg^{-1}(\frac{2t}{\Delta})$ to $\tilde{H} = \left(\begin{smallmatrix} \alpha & 0 \\ 0 & \beta \end{smallmatrix}\right)$ with

$$\alpha = \tfrac{1}{2}(\Delta + \sqrt{\Delta^2 + 4t^2}); \qquad \beta = \tfrac{1}{2}(\Delta - \sqrt{\Delta^2 + 4t^2}) \tag{8}$$

the transformation from the original representation to the new representation is given by:

$$\begin{pmatrix} \tilde{x} \\ \tilde{y} \\ \tilde{z} \end{pmatrix} = \begin{pmatrix} \cos(2\theta) & 0 & \sin(2\theta) \\ 0 & 1 & 0 \\ -\sin(2\theta) & 0 & \cos(2\theta) \end{pmatrix} \begin{pmatrix} x \\ y \\ z \end{pmatrix}.$$

In the new representation, the evolution of the ensemble-averaged Bloch sphere variables is described by

$$\begin{pmatrix} \dot{\tilde{x}} \\ \dot{\tilde{y}} \\ \dot{\tilde{z}} \end{pmatrix} = \begin{pmatrix} \frac{-\gamma_{\rm dec}}{2}\cos^2(2\theta) & \sqrt{\Delta^2 + 4t^2} & \frac{-\gamma_{\rm dec}}{4}\sin(4\theta) \\ -\sqrt{\Delta^2 + 4t^2} & \frac{-\gamma_{\rm dec}}{2} & 0 \\ \frac{-\gamma_{\rm dec}}{4}\sin(4\theta) & 0 & \frac{-\gamma_{\rm dec}}{2}\sin^2(4\theta) \end{pmatrix} \times \begin{pmatrix} \tilde{x} \\ \tilde{y} \\ \tilde{z} \end{pmatrix}. \tag{9}$$

We can monitor the state of the qubit from the evolution of the moment z. The calculated results of ensemble-averaged evolution of the system state are plotted in figures 4–8 illustrating the influence of various parameters. When a particular parameter is chosen to vary in a plot, all other parameters in the figure are fixed.

4. Results and discussion

For the ensemble evaluation of the qubit state we use the approximate values of real Δ and t given by Kane [15],

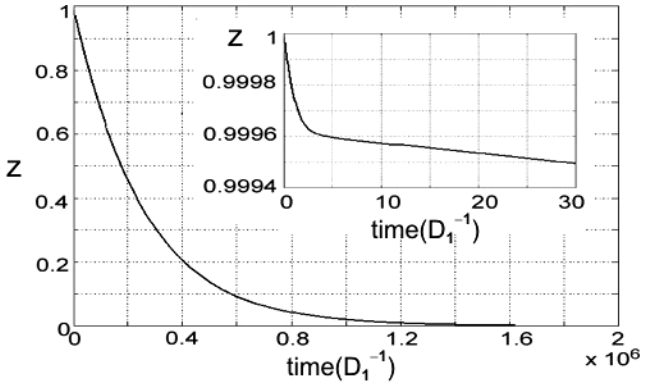

Figure 4. Locality of the electron at $D_0 = 0.5$, $\Delta = 0.1$ and $t = 10^{-4}D_1$.

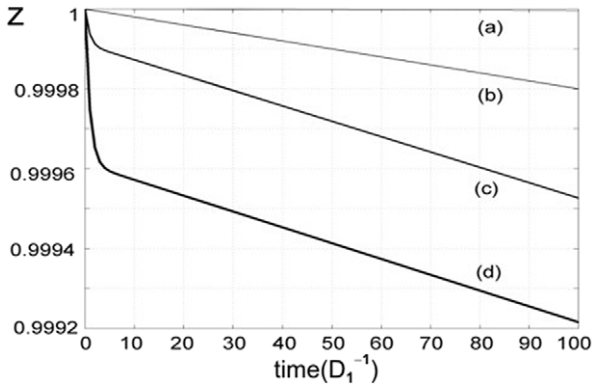

Figure 5. Influence of Δ: from the top $\Delta = 10, 5, 0.2, 0.1\ D_1$.

i.e. $\Delta/h = 110$ GHz and $2t/h = 1$ GHz. The values of the ratio of t/Δ in all plots are therefore chosen as 5×10^{-3}.

Figure 4 shows a typical evolution of the locality of the state. It is obvious that the system is not oscillating but deviates from the initial state to a mixed state as time approaches 'infinity', which is different from the coherent tunneling case. The inset gives enlarged details of the early stage, which shows a sharp deviation followed by a flatter slope. Figures 5–7 show the effects of the energy gap Δ, the coupling rate between the two dots t and the quiescent rate of current tunneling through the RD D_0, respectively.

In the plots, all parameters are normalized by the rate D_1. Both top lines (a) in figures 6 and 8 are very close to the top frame edge. As expected, we see that for larger Δ (figure 5(a)) and smaller t (figure 6(a)), the deviation is slower and the smaller background rate of the detector D_0 ((c) in figure 7), the better the measurement quality. The interesting feature in figure 7 is that with a small D_0, z shows a sharp first slope followed by a flatter second slope, which is a most desirable condition, as it may be interpreted as the state being distinguished quickly with less deviation from the initial state. Now we reach a question naturally: how would one judge the quality of a measurement? One parameter determining the quality of a measurement is the localization rate, which is related to the signal-to-noise ratio. The characteristic time is defined as the minimum time when the two possibilities

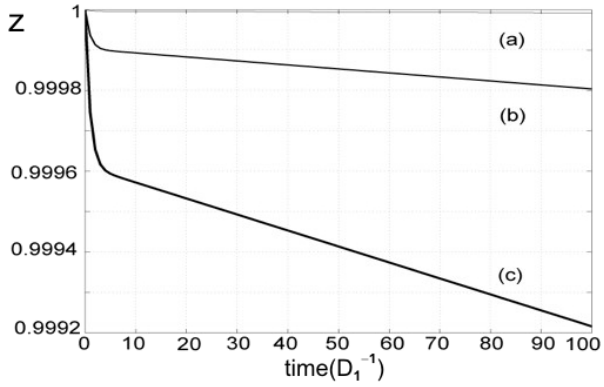

Figure 6. Influence of t, from the top: $t = 0.1 \times 10^{-4}, 10^{-4}, 5 \times 10^{-4}D_1$.

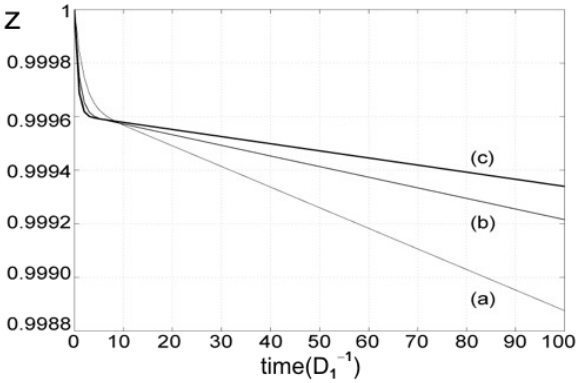

Figure 7. Influence of D_0: from the top $D_0 = 0, 0.5, 1D_1$.

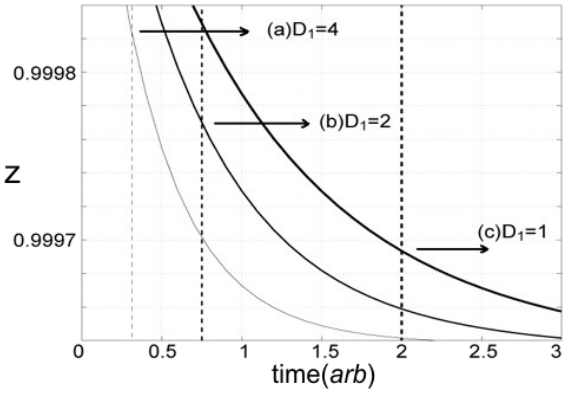

Figure 8. Comparison of measurement quality for various D_1. The dashed lines are the corresponding characteristic times.

of the electron locality are distinguishable. In our system it is given by $T = (2D_0 + D_1)/D_1^2$, which is twice the inverse of the localization rate [4]. Within the characteristic time, the closer we are to the initial state and the better is the measurement. Figures 8 and 9 illustrate the comparisons of the measurement qualities with various parameter combinations. Figure 8 shows that the larger D_1 is (strong coupling between the qubit and the detector), the more sensitive is detection and the RD reads out the state of the qubit in a shorter time with less disturbance. In figure 9, D_0 and D_1 vary in their absolute

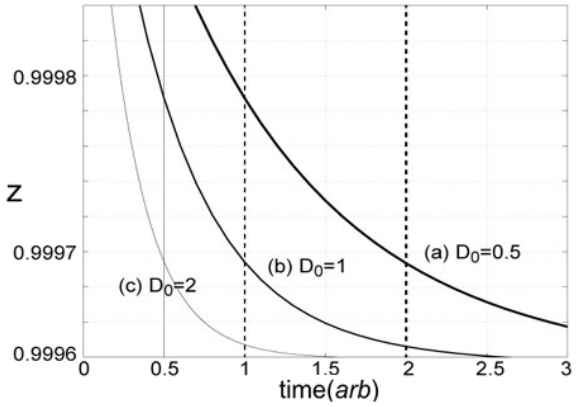

Figure 9. Comparison of measurement quality for different values of D_0 at a fixed ratio of $D_0/D_1 = 0.5$.

values at the fixed ratio of $D_0/D_1 = 0.5$. It is clear from the graph that the larger rates of RD (curve c) make better measurement and strong coupling is therefore preferred. All combinations of parameters we chose in the plots are based on Δ and t values initially from the real system in [15] and actually within reasonable ranges (around the same order of magnitude) corresponding to reported experiment values. (For example, RD current rate $D_1 \sim$ 10–100 GHz compared to 75 GHz in [11]; tunneling rate t from 0.01–1 GHz compared to 0.01 GHz [11] to 2.8 GHz [10].)

The above outcomes may provide reference for device designers when they tackle optimum selection of the parameters. For example, if the technology limits the reduction of the quiescent current of a non-ideal detector, one could increase the measurement tunneling rate D_1 by device designing or bias setting in experiments to compensate and achieve better measurement quality.

5. Summary

It has been suggested that we use mesoscopic electronic systems such as coupled quantum dots, superconducting junctions, and single spin-polarised electrons as qubits. We model the quantum measurement of the states of such systems using the theory of open quantum systems. The requirements to perform quantum calculations and a quantum measurement (readout) appear to contradict each other. During the manipulations the dephasing should be minimized, while a quantum measurement should dephase the state of the qubit as far as possible. We propose a measurement scheme to study the dynamics of the system. To guarantee the calculated evolution representing the state of a real physical system, we derive the Lindblad-form master equation. We calculate the conditional evolution of the states and the ensemble-averaged evolution of the states of the coupled quantum dots as the qubit. The results show the effects of various device parameters on the quality of the measurements. Most reported experimental measurements are limited by the finite bandwidths (device and amplifier circuit, etc) and fail to count very fast successive transitions within 100 μs [11]. To our knowledge there have been no experiment reports on continuous measurement of the electron location in a coupled-dot charge qubit such as the one we are modeling in this paper. While direct comparison with experimental results is unavailable, our model uses the parameters that are comparable with those of the relevant real experiments, as stated in section 4. Also the parameters used in this paper are normalized by rate D_1, which provides us with the flexibility to fit individual experimental sets as references. These may contribute to the device parameter selection and experimental designing of the readout processes of a solid-state quantum computer for better performance.

References

[1] Gurvitz S A 1997 *Phys. Rev.* B **56** 15215
Gurvitz S A *et al* 2003 *Phys. Rev. Lett.* **91** 66801
[2] Shninman A and Schhon G 1998 *Phys. Rev.* B **57** 15400
[3] Sun H B and Milburn G J 1999 *Phys. Rev.* B **59** 10748
Oxtoby N *et al* 2003 *J. Phys.: Condens. Matter* **15** 8055
[4] Wiseman H M *et al* 2001 *Phys. Rev.* B **63** 235398
[5] Korotkov A N 2001 *Phys. Rev.* B **63** 85312
[6] Jordan A N and Buttiker M 2005 *Phys. Rev. Lett.* **95** 220401
[7] Oxtoby N P *et al* 2006 *Phys. Rev.* B **74** 045328
[8] Luo J Y *et al* 2007 *Phys. Rev.* B **76** 085325
[9] Dong B *et al* 2008 *Phys. Rev.* B **77** 085309
[10] Petta R *et al* 2004 *Phys. Rev. Lett.* **93** 186802
[11] Fujisawa T *et al* 2006 *Science* **312** 1634
[12] Gustavsson S *et al* 2008 *Appl. Phys. Lett.* **92** 152101
[13] Carmichael H 1993 *An Open Systems Approach to Quantum Optics* (Berlin: Springer)
Wiseman H M and Milburn G J 1993 *Phys. Rev.* A **47** 1652
[14] Lindblad G 1976 *Commun. Math. Phys.* **48** 119
[15] Kane B E *et al* 2000 *Phys. Rev.* B **61** 2961